

Location, location, location (and density) of gap junctions in multi-compartment models

Fernanda Saraga and Frances K. Skinner

*Toronto Western Research Institute, University Health Network
and University of Toronto*

Abstract

Interneuronal networks are important in mediating several rhythmic brain states. Their interconnections include dendritic gap junctions which can give rise to various network patterns depending on their location and density. We develop full and reduced (two-compartment) multi-compartment models of hippocampal basket cells and examine two-cell networks of them. The location and density of the gap junctions determine if and when synchronous and phase-locked patterns arise. Comparison of the full and reduced network models allows us to obtain biological quantification of gap junction conductance values in the reduced models.

Introduction

Gap junctions (GJs) are well-known portals of electrical, intercellular communication [3, 30]. They consist of twelve connexin (Cx) proteins, six of which form hemichannels or connexons. Neuronal GJ proteins (Cx 36) have been identified and Cx36 knockout mice have been created [6, 14, 21]. Furthermore, there is direct anatomical evidence for the presence of GJs between the dendrites of basket cells in hippocampus [8].

A common cortical infrastructure appears to be interneuronal networks of basket cells connected by both inhibitory synapses and GJs [2, 7, 8, 9, 10, 11, 19]. These interneuronal

networks play central roles in mediating rhythmic patterns of different frequencies that are associated with various behavioural states [4, 29]. The importance of GJs in mediating various brain rhythms is currently an intense area of investigation using *in vivo* and *in vitro* preparations, knockout mice and modelling studies [6, 14, 16, 22, 24, 26]. Despite this, it is far from clear how GJs contribute to the output produced by interneuronal networks. To understand the potential role(s) of GJs in normal (and pathological) states, as expressed in brain rhythms, we need to understand how the location and density of GJs give rise to different dynamic network patterns.

Theoretical and modelling studies using simple neuronal caricatures clearly show that the effects of GJ-coupling are not straightforward. Synchronous, anti-phase, phase-locked and bistable patterns can be produced in GJ-coupled networks depending not only on GJ strength, but also details of the spike shape and frequency [1, 5, 15, 23]. To gain further insight from these studies, we need to be able to attribute biological quantification of the parameters used in them.

In this paper we develop two multi-compartment models of a hippocampal basket cell. The first model is a full multi-compartment model based on morphological data in the literature and on the web. The second is a two-compartment model which represents a phenomenological reduction of the full model. We build two-cell networks of these models coupled via GJs and examine their network dynamics. The location and density of the GJs determines if and when synchronous and phase-locked patterns arise. By comparing the full and reduced network models we can obtain biological quantification of GJ conductance values in the reduced two-compartment models. In this way, theoretical insights obtained using simpler models can be interpreted in a more biologically relevant fashion.

Models and Methods

Full multi-compartment model: A 372-compartment model was built using NEURON [13]. It is based on a hippocampal basket cell morphology taken from [12] and <http://www.koki.hu/~gulyas/calcells> and has a surface area of $18,069 \mu m^2$ (Figure 1 A, B). The dendrites are passive and the soma contains I_{Na} , I_K and I_L , (sodium, potassium HH-like currents and leak currents respectively), with kinetics taken from [28]. The conductances for these channels were modified from [17, 18] in order to match electrophysiological responses and passive properties of hippocampal basket cells [20, 27] ($g_{Na} = 184 mS/cm^2$, $g_K = 140 mS/cm^2$, $C_m = 0.8 \mu F/cm^2$, $R_a = 200 \Omega cm$, $g_L = 2.45 \times 10^{-5} S/cm^2$, $E_L = -60 mV$, using the input resistance $R_{in} = 245 M\Omega$, and membrane time constant, $\tau_m = 30 ms$). Each basket cell model spontaneously fires at $12.7 Hz$ with an amplitude of $110 mV$ and an after-hyperpolarization (AHP) of $\sim 18 mV$.

Reduced multi-compartment model: A two-compartment model (representing the soma and dendritic tree) was constructed (Figure 1 C) using the following equations for a given cell:

$$C \frac{dV_S^i}{dt} = I_{app} - I_{Na} - I_K - I_L - g_c (V_S^i - V_D^i) \quad (1)$$

$$C \frac{dV_D^i}{dt} = -I_L - g_c (V_D^i - V_S^i) - g_{gap} (V_D^i - V_D^j) \quad (2)$$

where C is capacitance, $V_{S/D}$ is the voltage in the soma (S) or dendrite (D), t is time, I_{app} is applied external input, and g_c is the coupling between somatic and dendritic compartments. Passive properties were taken from the full multi-compartment model and intrinsic currents were taken from [28] where the sodium and potassium conductances were doubled. The last term in equation (2) is included only when two-cell networks coupled with GJs are being considered,

where g_{gap} is the GJ conductance and i, j are neuron indices that refer to different neurons. The location of the GJs on the dendritic tree is determined by the g_c parameter (see below).

Two-cell networks: Two-cell (homogeneous) networks of model cells coupled by GJs were constructed. We selected three different locations on the dendritic tree: proximal ($\sim 100 \mu m$ from soma), middle ($\sim 200 \mu m$) and distal ($\sim 400 \mu m$), and different physiologically plausible densities of GJs were inserted. These values ranged from 10-3000 pS and are based on a unitary conductance value of 10-300 pS and 1-10 GJs per electrical connection [10, 25]. For each selected location, we created a two-compartment model in which g_c was adjusted to match the attenuated spike heights seen at the particular dendrite location in the full model. (Note that this does not account for the degree of attenuation along the dendritic tree as seen in the full model). Networks of these reduced model cells are taken to correspond to GJs being located at the selected site in the full model. Three different intrinsic frequencies as determined by I_{app} were used: low ($\sim 22 Hz$), medium ($\sim 60 Hz$), and high ($\sim 150 Hz$). The process described in this paper is summarized in Figure 2.

Results

From previous modelling studies we know that with strong GJ-coupling, only synchronous behaviours will occur, but with weak GJ-coupling, bistable, anti-phase and other phase-locked patterns can arise [5, 15]. Our reduced network models produced such behaviours. Specifically, for a given location and intrinsic frequency, as g_{gap} increases, the network produces anti-phase, phase-locked (with decreasing phase lags) and synchronous output. Therefore, synchrony occurs with large g_{gap} , anti-phase firing with small g_{gap} , and phase-locked behaviours with intermediate g_{gap} . With higher intrinsic frequencies, larger g_{gap} is needed to achieve

synchrony and g_{gap} does not have to be as small as for anti-phase firing. The further away the GJs were “located” in the two-compartment model, the easier it was to obtain anti-phase firing.

With the full network models, we obtained results that were similar to the reduced network models, except that the full span of behaviours (synchrony to anti-phase) could not be obtained for a given location and frequency within the (generous) physiological ranges examined (see Table 1). For example, synchrony did not occur when GJs were located at farther locations and for higher intrinsic frequencies. Synchrony required stronger GJ-coupling (than for anti-phase firing) and occurred more easily in closer locations and with lower frequencies. Interestingly, unlike the reduced models, we found that the full network models could produce phase-locking with the same lag at both high and low GJ conductance values.

To biologically quantify GJ conductance values in the reduced network models, we examined phase-locked behaviours in which similar lags were present in the full and reduced models. We converted g_{gap} values in terms of surface areas and found that only when GJ conductances were in a 10-100 pS window were the reduced and full models quantifiably similar. If not, then g_{gap} in the reduced model was either too small (for smaller phase lag patterns which occurred at larger g_{gap}) or too large (for larger phase lags which occurred at smaller g_{gap}). This occurs because the two-compartment model does not adequately capture the attenuation and the changing input resistance due to GJ-coupling. For smaller g_{gap} , the former reason dominates whereas for larger g_{gap} , the latter reason takes over to cause g_{gap} in the reduced models to be inappropriate from a biologically quantifiable point of view. This is shown in detail in Figure 3 for some of the cases shown in Table 1. In general, GJ conductance values in

the two-compartment network models more closely approximate those in the multi-compartment network models for lower intrinsic frequencies and more proximal locations.

Conclusions

Our approach, as summarized in Figure 2, shows how we can obtain biologically quantifiable parameters for GJ-coupling in networks of reduced two-compartment models. From a physiological perspective, insight and analyses using the reduced models will be instructive directly. We estimate that to be within physiological values, one only needs to explore a two-fold range (from a phase-locked state) of GJ conductance values in the two-compartment models. This quantification should allow us: (i) to gain more from theoretical studies performed using “simpler” models in which biological quantification of parameter values is difficult, and (ii) to explore larger network dynamics in physiological relevant parameter regimes using reduced models. Furthermore, it will be interesting to investigate interneuronal network dynamics in which the coupling involves both GJ- and inhibitory coupling. Such investigations can be done in a biologically quantifiable fashion using the approach in this work and with the consideration of previous theoretical insights [15].

References

- [1] V.A. Alvarez et al., Proc. Natl. Acad. Sci. USA, 99 (2002) 4032-4036.
- [2] Y. Amitai et al., J. Neurosci., 22 (2002) 4142-4152.
- [3] M.V. Bennett, J. Neurocytol., 26 (1997) 349-366.
- [4] G. Buzsáki and J.J. Chrobak, Curr. Opin. Neurobiol., 5 (1995) 504-510.
- [5] C.C. Chow and N. Kopell, Neural Comput., 12 (2000) 1643-1678.

- [6] M.R. Deans et al., *Neuron*, 31 (2001) 477-485.
- [7] T. Fukuda and T. Kosaka, *Neurosci. Res.*, 38 (2000) 123-130.
- [8] T. Fukuda and T. Kosaka, *J. Neurosci.*, 20 (2000) 1519-1528.
- [9] M. Galarreta and S. Hestrin, *Nature*, 402 (1999) 72-75.
- [10] M. Galarreta and S. Hestrin, *Rev. Neurosci.*, 2 (2001) 425-433.
- [11] J.R. Gibson et al., *Nature*, 402 (1999) 75-79.
- [12] A. Gulyás et al., *J. Neurosci.*, 19 (1999) 10082-10097.
- [13] M. Hines and N.T. Carnevale, *Neural Comput.*, 9 (1997) 1179-1209.
- [14] S.G. Hormuzdi et al., *Neuron*, 31 (2001) 487-495.
- [15] T.J. Lewis and J. Rinzel, *J. Comput. Neurosci.*, 14 (2003) 283-309.
- [16] N. Maier et al., *J. Physiol.*, 541 (2002) 521-528.
- [17] M. Martina and P. Jonas, *J. Physiol.*, 505.3 (1997) 593-603.
- [18] M. Martina et al., *J. Neurosci.*, 18 (1998) 8111-8125.
- [19] C.J. McBain and A. Fisahn, *Nature Rev. Neurosci.*, 2 (2001) 11-23.
- [20] F. Morin et al., *J. Neurophysiol.*, 76 (1996) 1- 16.
- [21] J.E. Rash et al., *Proc. Natl. Acad. Sci. USA*, 97 (2000) 7573-7578.
- [22] D. Schmitz et al., *Neuron*, 31 (2001) 831-840.
- [23] A. Sherman and J. Rinzel, *Proc. Natl. Acad. Sci. USA*, 89 (1992) 2471-2474.
- [24] F.K. Skinner et al., *J. Neurophysiol.*, 81 (1999) 1274-1283.
- [25] M. Srinivas et al., *J. Neurosci.*, 19 (1999) 9848-9855.
- [26] R.D. Traub et al., *Proc. Natl. Acad. Sci. USA*, 100 (2003) 1370-1374.
- [27] J.A. van Hooft et al., *J. Neurosci.*, 20 (2000) 3544-3551.
- [28] X.-J. Wang and G. Buzsáki, *J. Neurosci.*, 16 (1996) 6402-6413.

- [29] M. A. Whittington et al., Intl. J. Psychophysiol., 38 (2000) 315-336.
- [30] G. Zoidl and R. Dermietzel, Cell Tissue Res., 310 (2002) 137-142.

Biosketches



Fernanda Saraga is currently working on her Ph.D. at the University of Toronto. She graduated from the University of Toronto (B.Sc. – Physics and M.Sc. – Physiology). She is interested in creating computational models of inhibitory interneurons to understand their complex role in signal generation.



Dr. Frances Skinner is a Senior Scientist in the Toronto Western Research Institute, University Health Network, with appointments in Medicine (Neurology), Physiology and Biomedical Engineering at the University of Toronto. She graduated from the University of Waterloo (B.Math.) and Toronto (M.A.Sc., Ph.D.) and did 4 years of postdoctoral work in Boston and California. In general, she enjoys collaborative work and is interested in cellular-based mechanisms underlying neuronal network dynamics.

Figure Legends

Figure 1. **A** Hippocampal CA1 basket cell morphology **B** 372-compartment model built using NEURON **C** Schematic of reduced two-compartment model.

Figure 2. Protocol for an ad-hoc reduction of a multi-compartment model to a two-compartment model and quantification of GJ conductances in two-cell networks of the reduced models.

Figure 3. *Top:* Phase lag vs. GJ conductance values in reduced network models for different frequencies and locations. Conductance values have been converted based on surface area and location in 372-compartment model. Boxed areas refer to phase-locked behaviour obtained in the full network models. *Bottom:* Plots of the correcting factor for different locations and frequencies. This factor is the number that the conductance in the reduced models need to be multiplied by to obtain similar behaviour as in the full model.

Figure 1

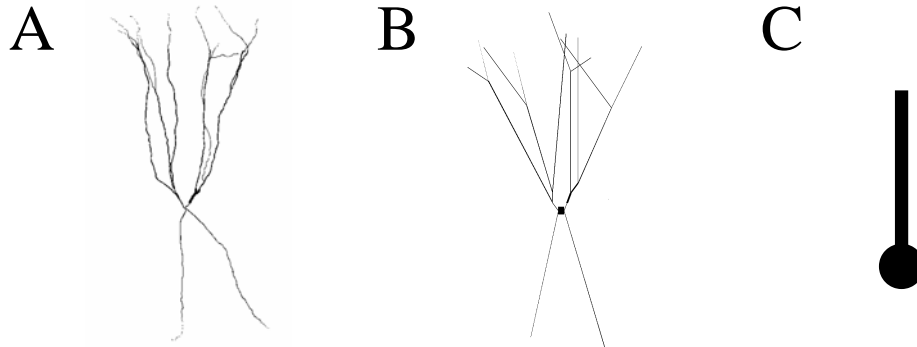


Figure 2

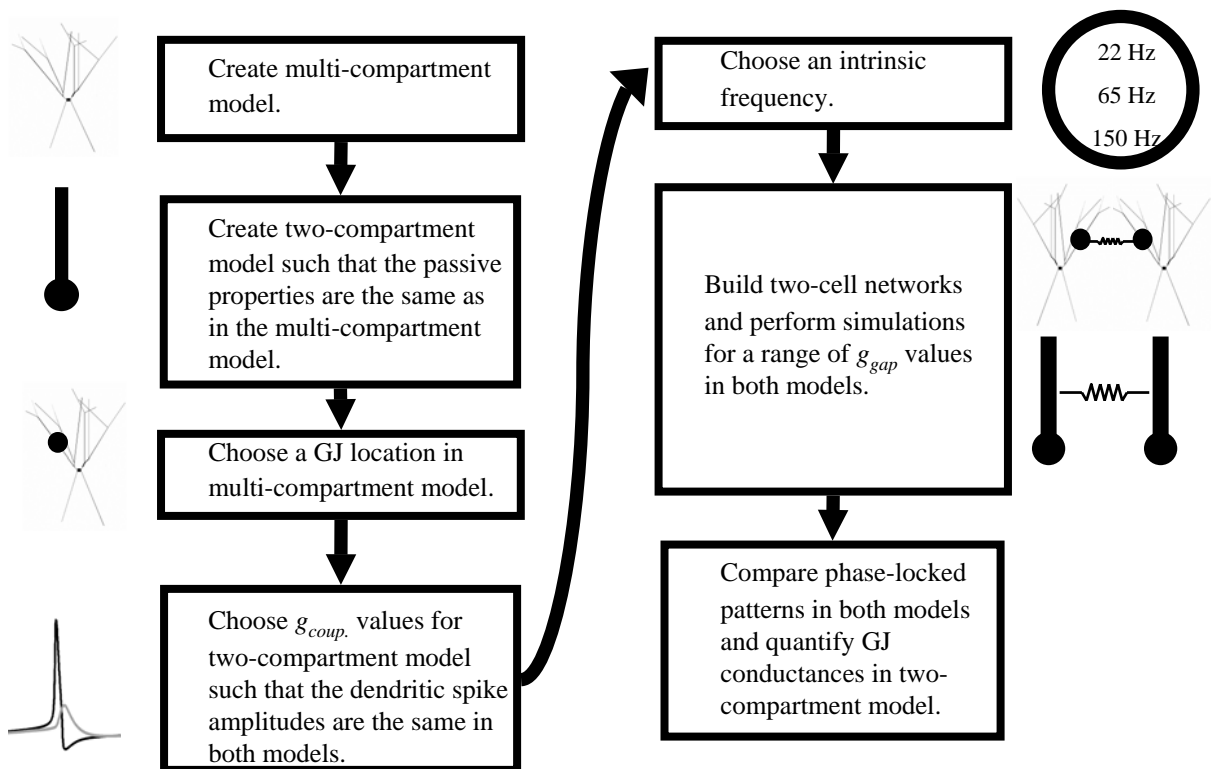
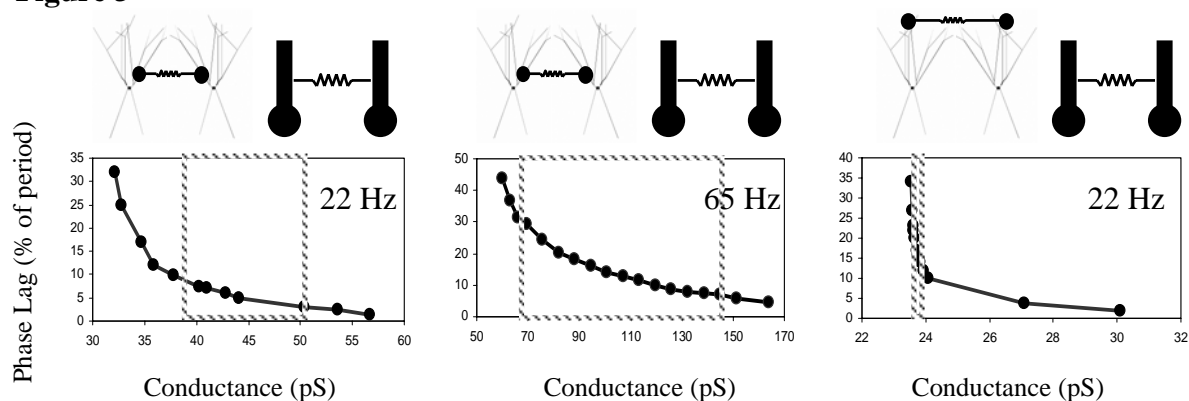
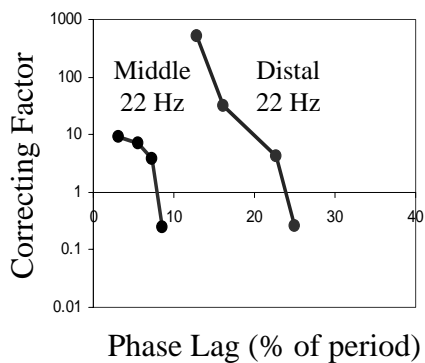


Figure 3



Different Locations



Different Frequencies

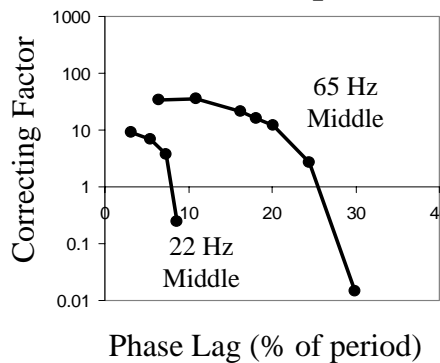
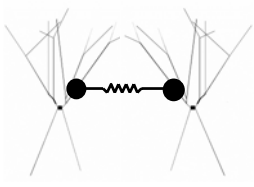
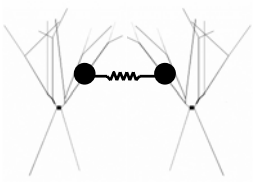
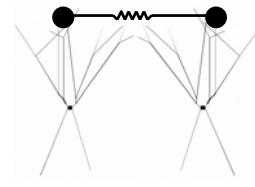


Table 1. Multi-compartment model results for proximal, middle and distal GJ locations.

Intrinsic Frequency of each model cell			
22 Hz	<i>Synchrony</i> : for all values	<i>Phase-locked</i> : < 450 pS <i>Synchrony</i> : > 450 pS	<i>Phase-locked</i> : < 200,000 pS <i>Anti-phase</i> : > 200,000 pS
65 Hz	<i>Synchrony</i> : for all values	<i>Phase-locked</i> : < 5000 pS <i>Synchrony</i> : > 5000 pS	<i>Anti-phase</i> : for all values
150 Hz	<i>Synchrony</i> : for all values	<i>Anti-phase</i> : for all values	<i>Anti-phase</i> : for all values